REPORT DOCUMENTATION PAGE

AFRL-SR-AR-TR-04-

0583

1. REPORT DATE (DD-MM-YYYY)	2. REPORT TYPE	
11/09/2004	Final Report	1 October 2001 - 31 March 2004

4. TITLE AND SUBTITLE

"Photosynthetic Complexes: Molecularly Activated Bioswitches and Agents for Light Powered Molecular Circuitry"

5a. CONTRACT NUMBER

F49620-01-1-0559

5b. GRANT NUMBER

5c. PROGRAM ELEMENT NUMBER

6. AUTHOR(S)

(a) Stephen R. Forrest
(b) Marc Baldo

5d. PROJECT NUMBER

5e. TASK NUMBER

5f. WORK UNIT NUMBER

7. PERFORMING ORGANIZATION NAME(S) AND ADDRESS(ES)

(a) Princeton University, Princeton, NJ
(b) Massachusetts Institute of Technology, Cambridge, MA

ME

8. PERFORMING ORGANIZATION REPORT NUMBER

9. SPONSORING/MONITORING AGENCY NAME(S) AND ADDRESS(ES)

Air Force Office of Scientific Research
4015 Wilson Blvd Room 713
Arlington, VA 22203-1954

10. SPONSOR/MONITOR'S ACRONYM(S)

11. SPONSOR/MONITOR'S REPORT NUMBER(S)

12. DISTRIBUTION/AVAILABILITY STATEMENT

Distribution Statement A: unlimited

13. SUPPLEMENTARY NOTES

14. ABSTRACT

This program was directed at demonstrating functional optoelectronic devices by contacting individual, highly photoactive molecules of biological origin. This 2 phase program (each phase duration of 1 year) successfully addressed the fundamental engineering issues associated with the application of protein/molecular aggregates to electronic devices: purification of the complexes, and their interconnection to conventional bulk organic circuitry. We demonstrated a molecular power source using a single antenna complex extracted from a biological photosynthetic unit. To exploit the optimization of photosynthesis, we have demonstrated, for the first time, the solid state integration of photosynthetic complexes in solar cells. The internal quantum efficiency of the first generation of devices is estimated to be 12%.

15. SUBJECT TERMS

16. SECURITY CLASSIFICATION OF:			17. LIMITATION OF ABSTRACT	18. NUMBER OF PAGES	19a. NAME OF RESPONSIBLE PERSON
a. REPORT	b. ABSTRACT	c. THIS PAGE		15	Stephen Forrest
					19b. TELEPHONE NUMBER (Include area code) 609-258-4532

Photosynthetic complexes:

Molecularly activated bioswitches and agents for light powered molecular circuitry

Stephen Forrest, Princeton University, Princeton, NJ 08544

Marc Baldo, Massachusetts Institute of Technology, Cambridge, MA

Abstract

This program was directed at demonstrating functional optoelectronic devices by contacting individual, highly photoactive molecules of biological origin. This 2 phase program (each phase duration of 1 year) successfully addressed the fundamental engineering issues associated with the application of protein/molecular aggregates to electronic devices: purification of the complexes, and their interconnection to conventional bulk organic circuitry. We demonstrated a molecular power source using a single antenna complex extracted from a biological photosynthetic unit. To exploit the optimization of photosynthesis, we have demonstrated, for the first time, the solid state integration of photosynthetic complexes in solar cells. The internal quantum efficiency of the first generation of devices is estimated to be 12%.

Photosynthetic complexes:

Molecularly activated bioswitches and agents for light powered molecular circuitry

Project Summary

The ability to arbitrarily position and to make electrical contact to individual molecules is crucial to the progress of molecular electronics. One possible solution to this problem may be found in nature, where space-filling protein scaffolds are used to control the exact placement and orientation of optically and electronically active molecular components. This 2 phase program (each phase duration of 1 year) successfully addressed the fundamental engineering issues associated with the application of protein/molecular aggregates to electronic devices: purification of the complexes, and their interconnection to conventional bulk organic circuitry. Our objective was also to demonstrate a molecular power source using a single antenna complex extracted from a biological photosynthetic unit. Due to the remarkable energy-sharing properties of antenna complexes it is possible to quench more than 400 photosynthetic dye molecules with a single molecular trigger. To exploit the optimization of photosynthesis, we have demonstrated, for the first time, the solid state integration of photosynthetic complexes in solar cells. The internal quantum efficiency of the first generation of devices is estimated to be 12%.

Detailed Description

(i) Choice of materials

There are two general categories of photosynthetic complexes. The most primitive belong to bacteria that do not generate oxygen as part of the photosynthetic process. These complexes are known as light harvesting (LH) complexes. The second, more sophisticated set of complexes, belong to oxygenic bacteria and higher plants. The constituent components of oxygenic photosynthesis are known as photosystem (PS) I and II, and in combination they generate oxygen in addition to storing energy as carbohydrate.

We employed two relatively well-characterized biomolecular complexes, LH2 and PSI. As shown in Fig. 1, LH2 is part of the photosynthetic machinery of the primitive purple bacteria

Photosynthetic Machinery of purple bacteria

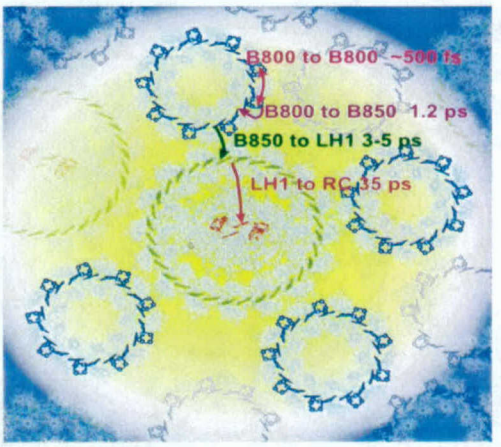

V. Sundstrom, *et al.*, J. Phys. Chem. B. **103**, 2327-2346 (1999)

Fig. 1. The structure of a light harvesting complex, showing the many dye molecules that are precisely positioned to absorb sunlight and transfer the energy to a dissociation center.

(*Rhodopseudomonas acidophila*). On the periphery and shown in blue, are the light harvesting complex LH2 complexes, these gather energy and transfer it to the central LH1 complex shown in green, which in turn, transfers the energy to a reaction center (RC) shown in red. A side view of an LH2 complex is shown in Fig. 2. These complexes only act as antennas. They are biologically optimized to funnel energy to the reaction center within 100ps with an overall quantum yield of 98%.[2,3] They consist of concentric

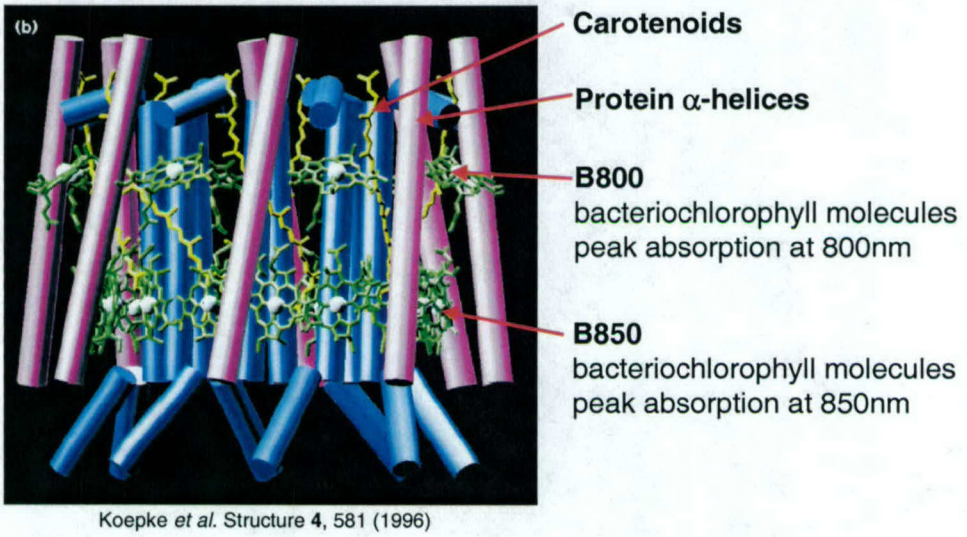

Fig. 2. A side view of an LH2 complex. Note the concentric rings of bacteriochlorophyll molecules shown in green.

rings of bacterio-chlorophyll molecules supported by protein pillars. The protein serves several purposes: it gives the photosynthetic unit its rigidity, fixes the pigments at their positions, and provides a heat sink for excess energy.[3] As shown, antenna complexes such as LH2 are archetypal molecular circuits; their operation relies on the positioning of the constituent bacteriochlorophyll molecules with a resolution that is beyond the capabilities of other lithography techniques. In nature they are formed by 'guided' self-assembly. Proteins are built following the genetic code of the organism. Once formed, they fold, forming a template for the self-assembly of bacteriochlorophyll molecules. These are positioned in two rings. The outer ring absorbs predominantly at $\lambda = 800$ nm, and is known as B800. The inner ring exhibits closer interactions between bacteriochlorophyll molecules, lowering the energy. It absorbs predominantly at $\lambda = 850$ nm, and is known as B850.

LH2 contains only two proteins and is probably the simplest photosynthetic complex, and also the most robust. It is therefore ideally suited to initial experimental investigations, especially deposition techniques and demonstrations of electrical integration. In contrast, Photosystem I (PSI) originating from the oxygenic purple bacterium *Synechococcus Elongatus* is significantly more complex. It performs the light gathering function of LH2 but also includes a reaction center that dissociates excited states into charges. PSI may be obtained from higher order plants as well as cyanobacteria. However, cyanobacterial PSI has proved more robust to experimental

analysis.[4] The structure as determined by Schubert, *et al.*[1] is shown in Fig. 3. PSI preferentially forms trimers. Charge generation occurs at the reaction center in the center of each PSI monomer (shaded yellow, Fig. 4). Approximately 100 chlorophyll molecules surround the reaction center.[1] These molecules absorb light and channel it to the center, acting as a highly efficient antenna. There are also 15-25 carotenoid molecules that absorb light at wavelengths where the chlorophyll molecules possess low sensitivity.[1] The carotenoids protect the structure against oxidation by quenching the formation of singlet oxygen.[1] PSI may exist on its own or in combination with additional light harvesting complexes, thereby enhancing its absorption under low light levels.

After absorption of a photon, the energy is channeled to the primary electron donor at the lower (lumen) surface of the complex. Following exciton dissociation, the electron is transferred through three Fe_4S_4 clusters to the opposite (stroma) surface. The result is an electron on the stroma surface and a hole on the lumen surface.[1] Due to the

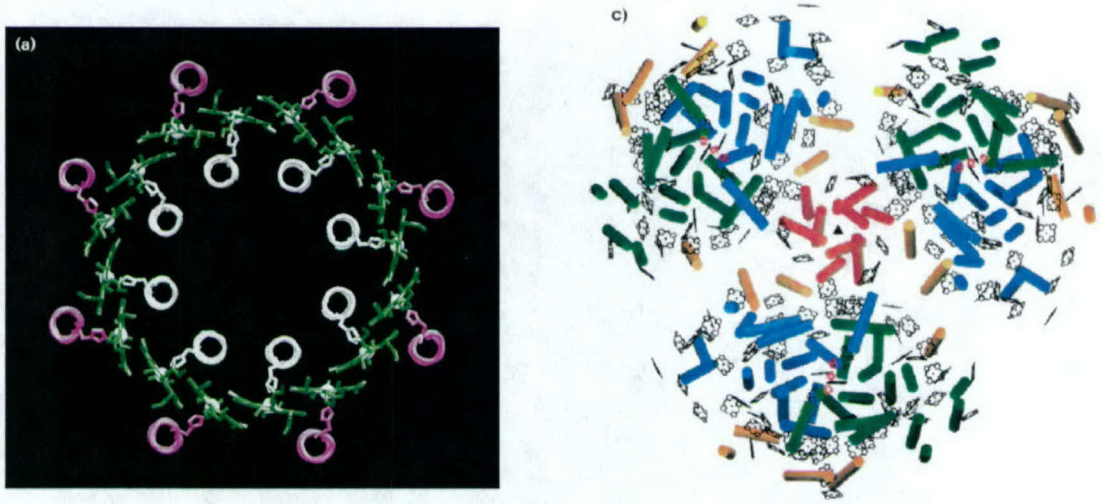

Koepke *et al.* Structure **4**, 581 (1996) Schubert *et al.* J. Molecular Biology **272**, 741 (1997)

Fig. 3. A cross section of the B850 ring in LH2 (left) compared with the structure of the PSI trimer (right). Note the enormous difference in sophistication. This is reflected in the additional functionality of PSI, which performs the antenna role of LH2 but also dissociates the absorbed light into charges. Note also the three red iron-sulfur complexes visible in the center of each PSI monomer. These participate in electron transfer after the initial exciton dissociation.

directed nature of electron transfer, it is necessary that the complexes possess the correct orientation when deposited on a substrate. Techniques for achieving this are discussed in Sec. (iii) below.

(ii) Bulk photovoltaic device structures

Photosynthetic complexes have been biologically optimized to convert incident radiation in electrical energy. In a typical PSI complex, absorbed photons are harvested within 100 ps with an overall quantum yield of 98%.[1] Photovoltages of 1 V are generated across the complex and the power conversion efficiency is approximately 40%.[1] Natural

biomolecular complexes exceed the efficiencies of even the best artificial photovoltaic devices (*c.f.* Si < 30%). This performance advantage results from millions of years of evolutionary optimization and provides the motivation for integrating bio complexes with

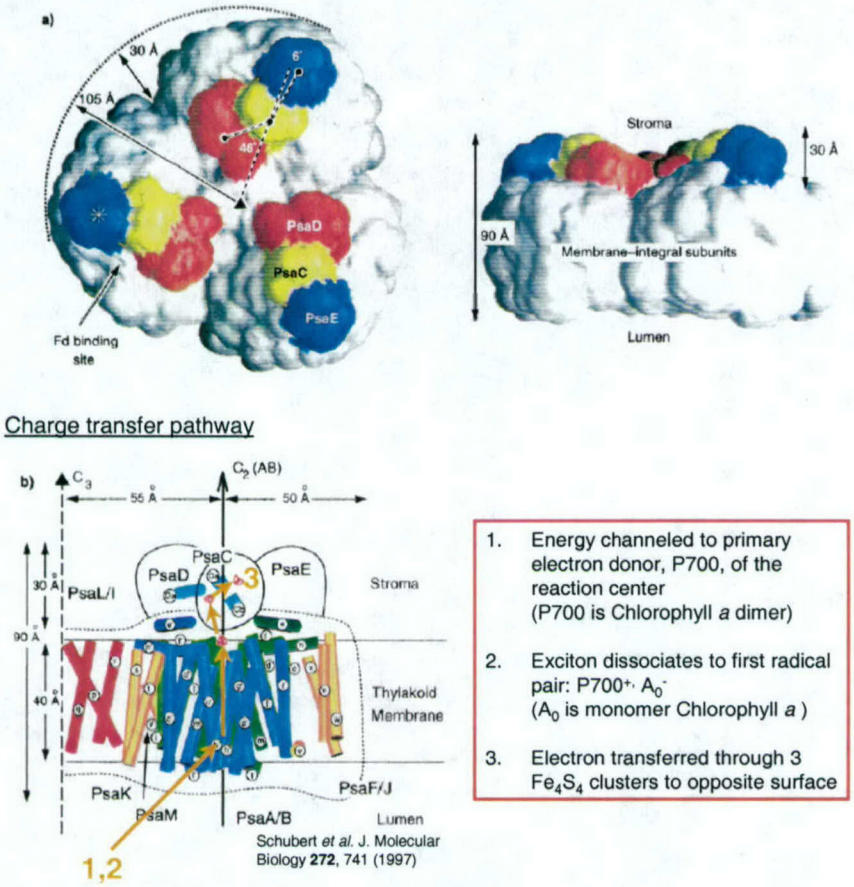

Fig. 4. (a) A top view and side views of a PSI complex from *Synechococcus Elongatus*. The process of charge dissociation is shown in (b). After the absorption of a photon, an electron is transferred to the stroma surface and the hole remains on the lumen surface. Note the three red iron-sulfur complexes on the stroma surface and also the protein, PsaD. This protein may be used to bind PSI to a substrate (see Sec. iv). From Schubert, *et al.*[2]

electronic devices.

But electrical integration with photosynthetic complexes also enables new device architectures. Designs of novel bio-PVs may be drawn from nature, and there are two particularly relevant principles of natural photosynthetic machinery. Firstly, natural complexes are designed to direct the flow of energy towards a particular location. Energy funnels such as these reduce losses associated with the random diffusion of excitons.

Secondly, by embedding photosynthetic complexes within a membrane, charge recombination is prevented, increasing power conversion efficiencies. We propose two novel devices based on these design rules.

(a) Guided energy organic PV

The essential processes occurring within a conventional organic PV are shown in Fig. 5. There is a tradeoff in the design of a conventional device between the absorption of

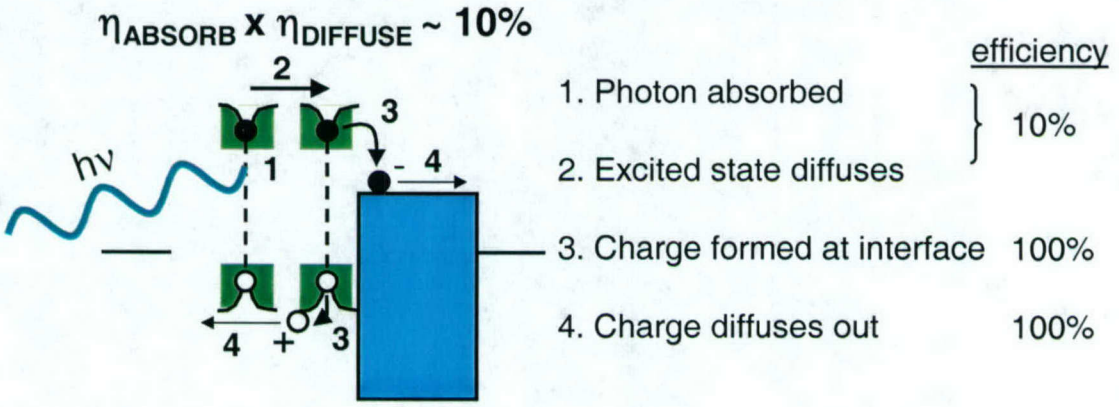

Fig. 5. The four main processes occurring in conventional organic PV cells. The biggest loss is the tradeoff between absorption (requires thick films) and excited state diffusion (losses minimized in thin films).

incident radiation and losses during exciton diffusion. In typical organic PVs, the exciton diffuses randomly until it either decays naturally, or is dissociated at an interface. If the morphology of the constituent organic films is carefully controlled, then diffusion may occur preferentially along one growth axis, increasing the diffusion length. But typically, films thicker than ~ 200Å exhibit substantial losses due to exciton decay. Thus, in thick devices, the absorption is large but many excitons decay before reaching the dissociation interface. This is the most important limitation to the power efficiency of many contemporary organic PVs.

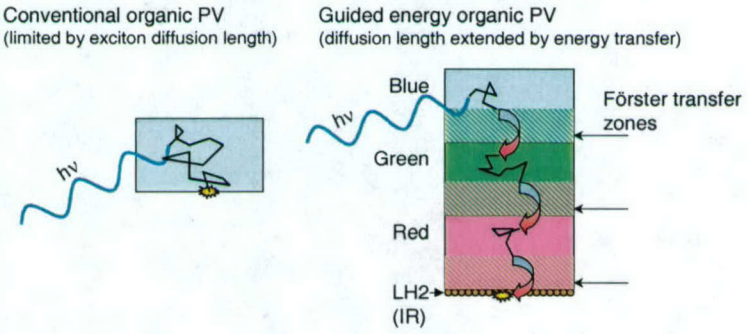

Fig. 6. A comparison of a conventional organic PV with a device where the energy is guided towards a photosynthetic complex LH2. Directing the flow of energy reduces losses due to random exciton diffusion and allows thicker absorption layers, increasing the overall power conversion efficiency.

Photosynthetic complexes offer a possible solution. Light harvesting complexes

from bacteria have extremely strong absorption in the infrared. In a PV cell containing photosynthetic material, the lowest energy states occur in the biological complexes. Thus, it is possible for absorbed energy to cascade down to complexes such as LH2. We have also shown that photons absorbed by complexes such as LH2 may generate photocurrent if the LH2 is deposited at an interface. Thus, LH2 is ideally used as part of an energetic funnel. Directed energy transfer using LH2 extends exciton diffusion lengths. In particular, non-radiative Förster transfer may be used to rapidly guide energy to the dissociation interface. In Fig. 6 the PV is structured into blue, green and red absorbing layers. Near the interfaces, energy may be transferred from one layer to the next by Förster transfer. Ultimately, energy is guided to the photosynthetic complexes at the charge dissociation interface. This allows the tradeoff between absorption and exciton losses to be substantially loosened, resulting in improvements to power conversion efficiencies.

(b) Membrane PV cells

In an alternate approach, nanostructured interfaces with extremely large surface areas may be used to increase the absorption of incident radiation. These cells do not require

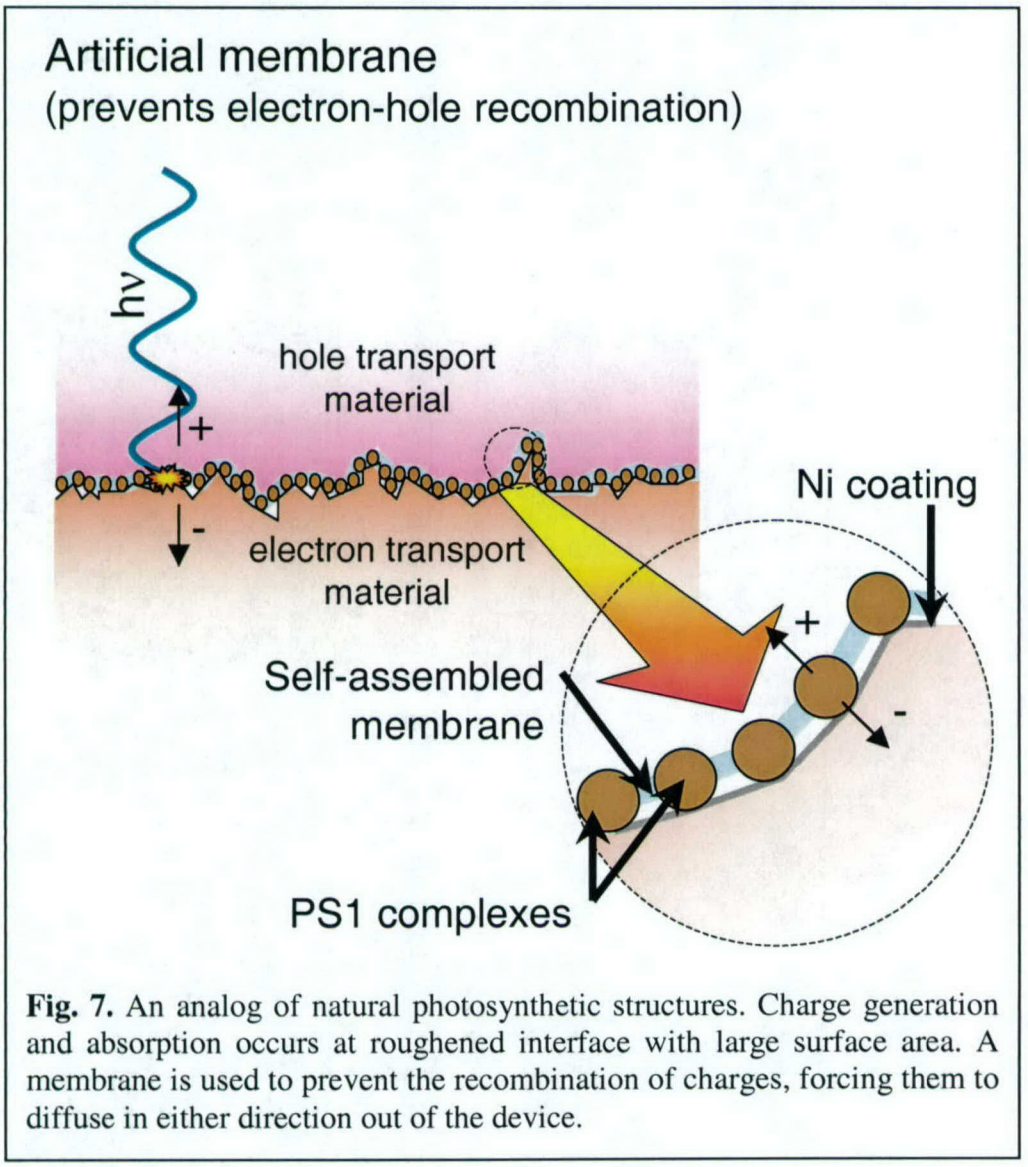

Fig. 7. An analog of natural photosynthetic structures. Charge generation and absorption occurs at roughened interface with large surface area. A membrane is used to prevent the recombination of charges, forcing them to diffuse in either direction out of the device.

exciton diffusion, since all excitons are absorbed at the dissociation interface. However, nanostructured PV cells are afflicted by losses because in the absence of an organic heterostructure there may be no barrier to charge recombination at the interface. (Ideally, all electrons and holes should diffuse out of a PV cell, generating photocurrent.)

Borrowing from structures employed in nature, electron-hole recombination may be eliminated by use of photosynthetic complexes linked by an insulating membrane. PSI is suited to this device because it operates *in vivo* within such a membrane. It may also be selectively absorbed on a surface using Ni-selective bonding, and the insulating membrane can be formed either using self-assembly or a Langmuir-Blodgett technique. No separate absorption layers are required because the interface has a large surface area. This device is an exact analog of the architectures employed in plants and bacteria.

(iii) Single complex devices

To maximize the capabilities of organic devices, we must aim for single molecule electronics. In the molecular regime, molecules are precisely positioned in circuits, intermolecular overlap is optimized and the nanometric scale lowers switching energies and transit times.

As discussed earlier, photosynthetic complexes are natural molecular circuits, whose constituent molecular components are supported by space-filling protein scaffolds. The functionality of protein complexes may eventually encourage the design of artificial proteins to support electronic circuits. But to demonstrate the potential of these structures and to study their properties, we must develop the technology to interface a single complex with conventional electronics, thereby opening the door to the entire range of natural and artificial protein-based systems.

We succeeded in sandwiching a single photosynthetic complex between metal contacts, forming a nanometric bio PV cell. When depositing metal contacts onto a single complex care must be taken not to disturb the protein scaffold. Techniques for fabricating metal contacts and patterning PSI on a substrate are discussed in the following sections.

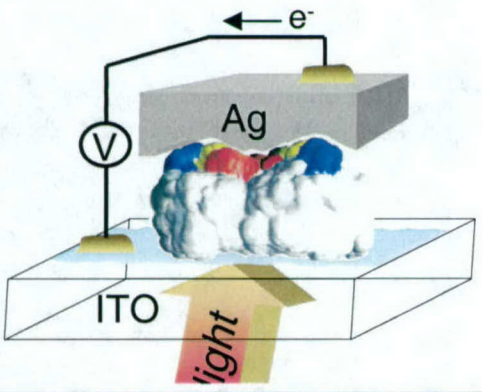

Fig. 8. A schematic of a single complex of PSI sandwiched between silver and transparent indium tin oxide. The ITO may be patterned using electron beam lithography, and lithographic definition of Ni may be used to control the self-assembly of recombinant PSI.

Fabrication of such a structure yields the following benefits:

(i) a nanometric integrable high efficiency PV for distributed power supply applications

(ii) a high speed, high resolution photodetector with 100% internal quantum efficiency

(iii) a unique platform for measuring the electrical and transient properties of biomolecular complexes

(iv) Deposition of biological complexes

The middle sections of LH2 and PSI are hydrophobic and *in vivo* they assist self-assembly of the complexes into a membrane. The stroma and lumen surfaces, however, are charged and hydrophilic. During isolation and purification, the membrane is dissociated using a detergent that also solvates and stabilizes the hydrophobic regions of the complexes. The stroma and lumen surfaces are unaffected. Thus, the complexes are typically obtained with relatively clean charge transfer surfaces. The work of Lee, *et al.*[7] determined that PSI complexes preferentially deposit from solution on hydrophilic surfaces with the lumen surface in contact with the substrate, *i.e.* the electron transport vector is perpendicular to the substrate, as is necessary for most devices. However, these workers estimated that only ~ 70% of PSI complexes self-assemble in the desired orientation. This is insufficient for high performance devices.

We have employed another self-assembly technique to fabricate monolayers of LH2. A schematic is shown in Fig. 11. By applying a small electric field across a solution of LH2, it is found that after approximately 1 day of electrostatic deposition and subsequent washing with water, a monolayer of LH2 is deposited on the positively charge surface. It is believed that residual impurities are deposited on the negatively charged surface, hence the method appears to have the additional advantage of purifying the solution.

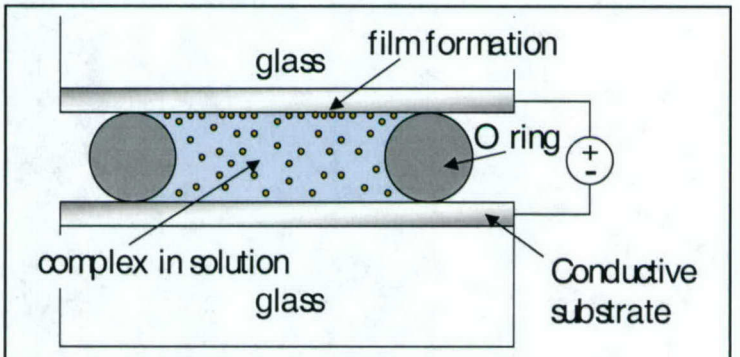

Fig. 9. A technique for the electrostatic deposition of LH2.

However, due to their inherent randomness neither of these self-assembly techniques are suited for the fabrication of sophisticated devices. For this application we will genetically engineer one of the constituent proteins in PSI to preferentially adhere to Ni. The targeted protein is PsaD on the stromal surface of PSI (see Fig. 3b). Recombinant PsaD can be engineered with a 6-histidine tag that selectively adheres to Ni.[8] In solution, PsaD in PSI is 'under constant maintenance', *i.e.* PsaD already incorporated into PSI is readily exchanged with PsaD in solution.[8] Thus, recombinant PsaD may be readily incorporated into native PSI by placing both recombinant PsaD and PSI together in solution.

Using this technique, deposition of PSI may be directed by prior patterning of Ni on a substrate using conventional lithographic techniques.

(v) Device fabrication

Electrical contact to protein complexes has been demonstrated using thermally evaporated protection layers comprising small molecules such as copper phthalocyanine (CuPc); see Fig. 10. The bulk devices described in Sec. (ii) will be fabricated using similar techniques.

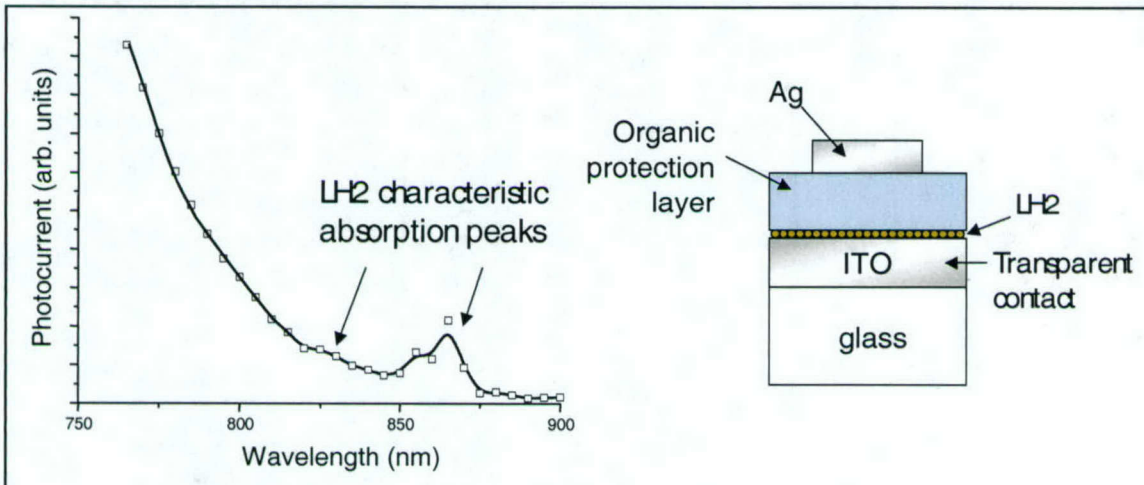

Fig. 10. A demonstration of electrical contact to LH2. Photocurrent characteristic of the absorption spectrum of LH2 is observed at ~800nm and 850nm.

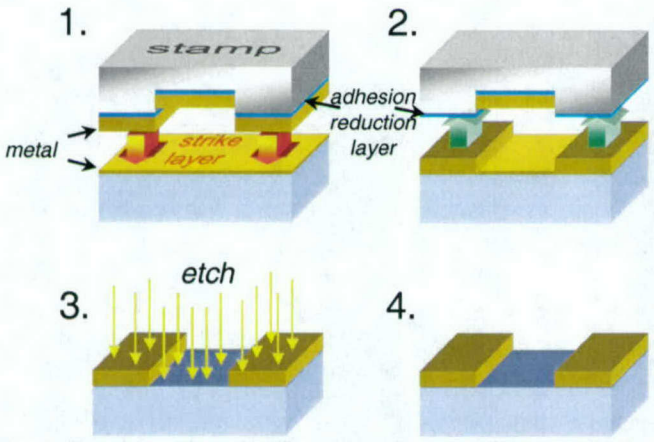

Fig. 11. The process of nondestructive contact formation. Prior to step 1, a thin layer (<50Å) of metal is deposited on the substrate using vacuum evaporation or sputtering. This 'strike' layer is sufficiently thin to minimize damage to any delicate features of the substrate. In step 1, a metal coated stamp is brought in contact with the strike layer. Metal is transferred at the points of contact. the substrate. In step 1, a metal coated stamp is brought in contact with the strike layer. Metal is transferred at the points of contact. Transfer may be enhanced by inserting an adhesion reduction layer between the stamp and its metal coating, and possibly eliminating the strike layer. After removal of the stamp in step 2, the patterned substrate is etched in step 3 and any exposed strike material is removed by Ar sputtering. The completed pattern is shown in step 4.

Metal contacts to single PSI complexes will be directly transferred by the ultrahigh resolution, non-damaging process of stamping by cold welding previously demonstrated in our laboratory.[9] A detailed description of the stamping process is shown in Fig. 11. The aim of the technique is the transfer of a metal film at the points of contact between a lithographically patterned stamp and a substrate at resolutions comparable to the diameter of the PSI complexes (~10nm). Transfer occurs if the substrate-metal adhesion exceeds adhesion forces between the stamp and the metal layer. To improve transfer, we have deposited adhesion reduction layers such as Teflon® between the stamp surface and the metal layer. In Fig. 14, we show a matrix with 100nm scale features generated with this technology. The dimensions of the stamped contacts will be defined by electron beam lithography.

Further results

1. We have demonstrated monolayer growth of LH2 using the electrodeposition technique described above. An example of one of the films is shown in Fig. 13, below.
2. We have realized photocurrent from LH2 by employing an organic protection layer; see Fig. 10 above. This demonstrates the feasibility of electronic integration with biomolecular complexes.
3. We have fabricated organic photovoltaic cells with 3.6% power conversion efficiencies. To our knowledge, these are currently the most efficient organic solid state photovoltaic devices.
4. We have fabricated photodetectors that overcome the relatively poor charge carrier mobilities in organic semiconductors, demonstrating bandwidths of up to 450MHz and external quantum efficiencies of ~ 80%.
5. We have developed a novel technique for non-destructive nanometric metal stamping. The method can be used for fabricating metal contacts to protein-structured biomolecular complexes. An example of a stamped structure is shown in Fig. 16, below.

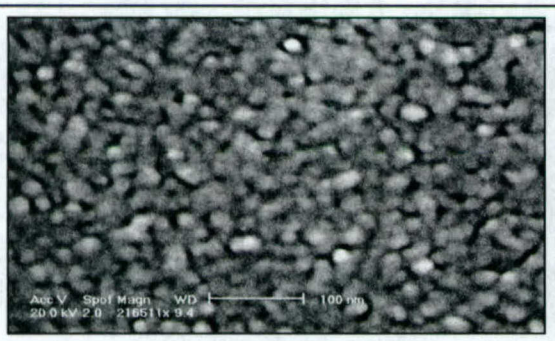

Fig. 13. A scanning electron micrograph of LH2 electrodeposited onto ITO. Note the ~10nm spherical complexes.

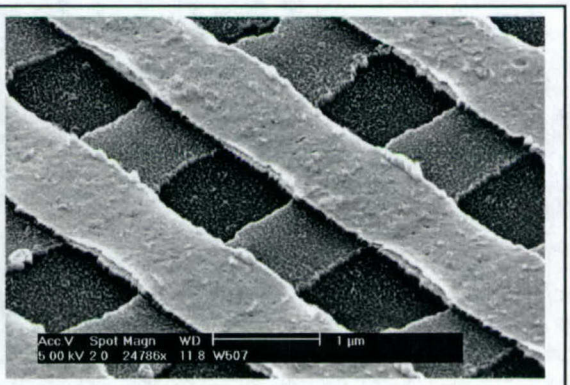

Fig. 14. An example of a structure made using metal stamping.

Stabilizing the complexes in an artificial environment is the key barrier to successful device integration. We achieved electronic integration of devices (see Fig. 15 and 16) by stabilizing an oriented, self-assembled monolayer of photosynthetic complexes using novel surfactant peptides, (see Fig. 17) and then depositing an organic semiconducting protective coating, required as a buffer to prevent damage to the complexes when depositing the top metal contact.

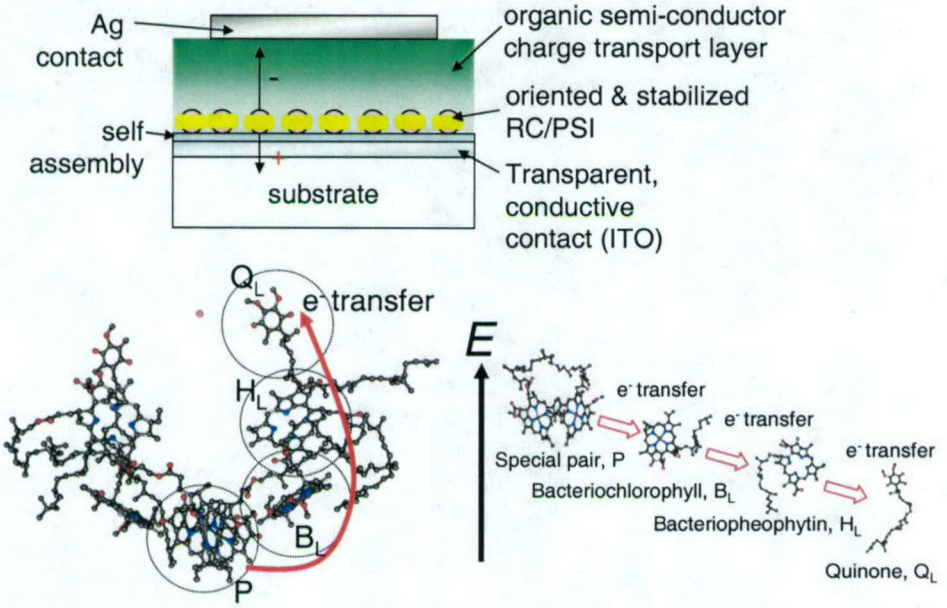

Fig. 15. ***(top left)*** *The structure of solid-state devices incorporating photosynthetic complexes.* ***(bottom left)*** *The internal molecular circuitry of a photosynthetic bacterial reaction center with the protein scaffold removed for clarity. The complex is only a few nanometers top-to-bottom. After photoexcitation, an electron is transferred from the special pair, P, to the quinone, Q_L. The process occurs within 200ps, at nearly 100% quantum efficiency, and results in the generation of a 0.5V potential.*

Successful integration is demonstrated by comparisons of the absorption spectrum and photocurrent spectra in Fig. 18.

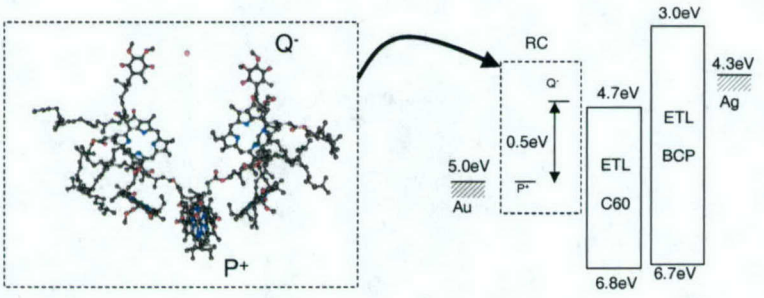

Fig. 16. *The device structure.*

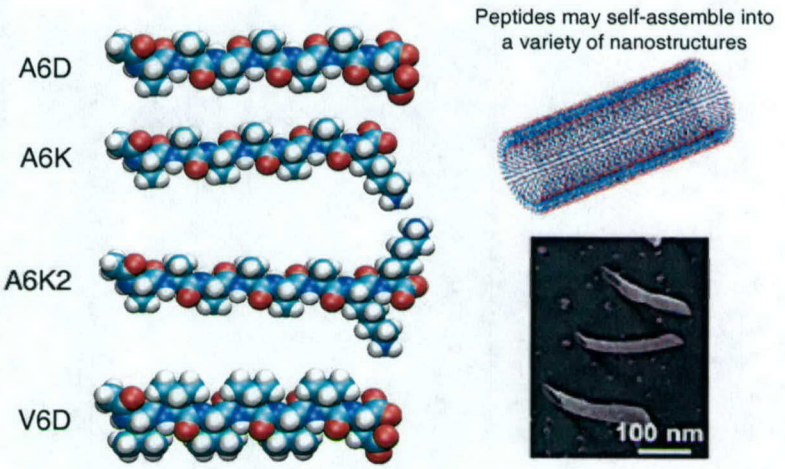

Fig. 17. *Stabilization during and after fabrication is the key to successful solid-state integration of biological molecular circuits. Here we show a selection of novel peptides, previously demonstrated to self-assemble in nanorods and nanovesicles. These enabled solid-state device integration.*

We have also demonstrated that it is possible to repair films of degraded photosynthetic complexes. The repair scheme is shown in Fig. 19. It exploits the ability to exchange protein subunits in the 13-protein aggregate Photosystem I (PSI). A tag was engineered on the subcomponent psaD. This can be exchanged with native psaD to bind PSI to the substrate. Bound PSI can be subsequently exhanged with new PSI to repair the surface.

Evidence for psaD-exchange mediated binding of PSI is shown in Fig. 20. To confirm the orientation of the PSI complexes we performed tapping mode-atomic force microscopy (TP-AFM) phase imaging in the intermittent contact mode and varied the potential

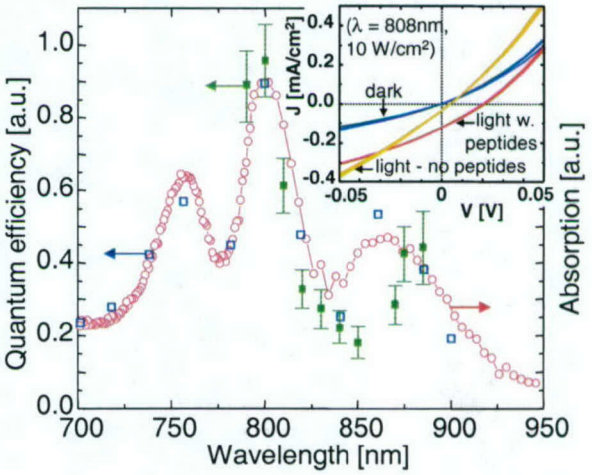

Fig. 18. *The photocurrent spectrum of solid-state photovoltaic devices employing bacterial reaction centers (RCs). A comparison between the photocurrent spectrum of solid-state (■) and wet electrochemical cell devices (□), and the solution absorption spectrum of the bacterial reaction centers (–o–), demonstrates that the observed photocurrent originates in the RCs.* ***Inset****: stabilization of RC complexes with A_6K/V_6D peptides improves the internal quantum efficiency of the devices to 12% under short circuit conditions.*

between the AFM tip and the ITO/Au substrate. The phase angle of the driven vibration of the cantilever in TM-AFM is related to the energy dissipated in the tip-sample interaction. Thus, phase images of biological materials provide a map of the dissipative part of the sample's mechanical response. When a potential is applied to the AFM tip, we can alter its mechanical interactions with polar or charged samples by, for example, aligning polar molecules in the electric field. Voltage-dependent phase scans of a typical

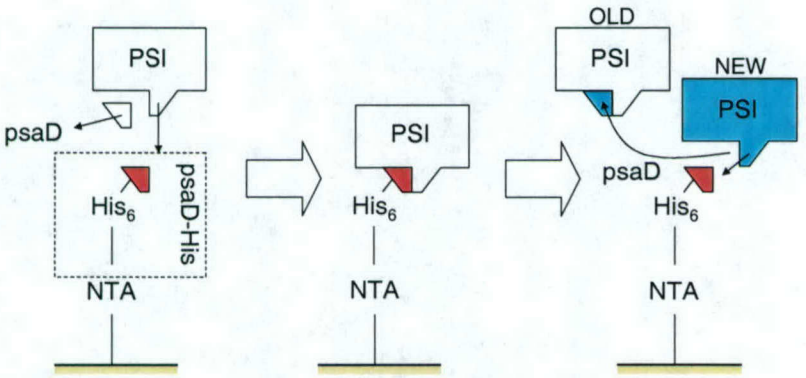

Fig. 19: *The process of repairing PSI films*

region of an assembled film are shown in Fig. 20. Phase scans taken at +1V and 0V show little difference, but phase scans taken at -1V exhibit the appearance of localized regions of increased phase. A subtraction of the –1V and 0V images is superimposed on the -1V image. The increase in phase in the -1V scan corresponds to an increase in the attractive forces between the tip and the sample and indicates the presence of a positive charge trapped on the surface of PSI, mostly likely at the special pair, P700. Thus, the voltage dependence of TM-AFM phase imaging is consistent with the rectifying characteristics of PSI in the orientation prescribed by self-assembly via exchange of psaD.

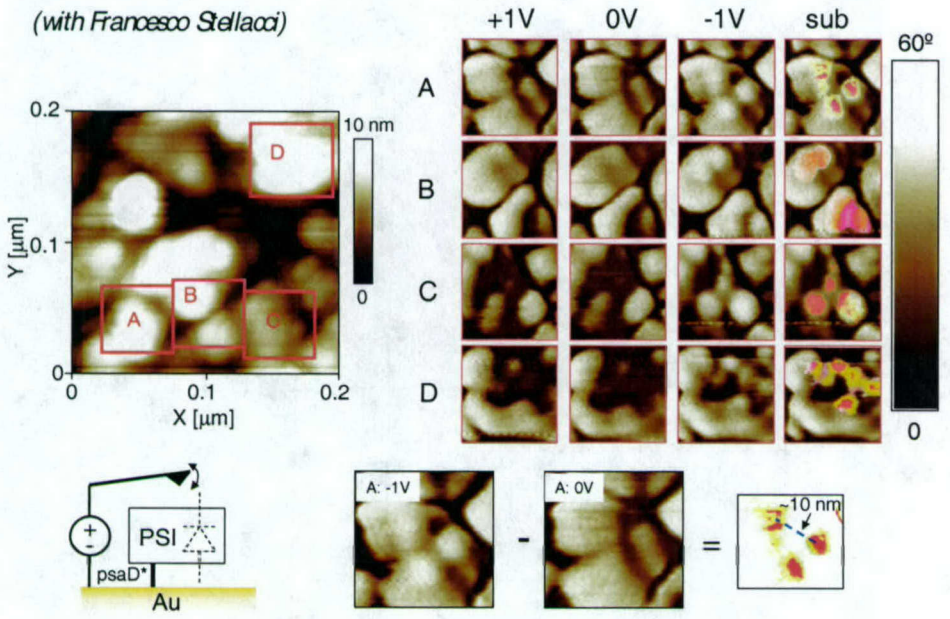

Fig. 20. *Characterization of self-assembled photosynthetic complexes by atomic force microscopy (AFM). The voltage dependence of a phase image of PSI particles is determined by applying a potential to the AFM tip. Note the phase changes in the –1V scan, relative to the +1V and 0V scans. Potential PSI particles are highlighted by superimposing a subtraction of the two images in (a) and (b) onto the -1V scan. The voltage dependence confirms that the rectifying PSI complexes are oriented with the P700 dimer face up. The phase profile of an assembled RC film showing a close*

References

1. '*Photoelectrochemical cells.*' M. Grätzel. Nature. **414**. 338-344 (2001).
2. '*High photovoltage multiple-heterojunction organic solar cells incorporating interfacial metallic nanoclusters.*' A. Yakimov and S.R. Forrest. Applied Physics Letters. **80**. 1667-1669 (2002).
3. '*Solid State Integration of Photosynthetic Protein Molecular Complexes.*' R. Das, P.J. Kiley, M. Segal, J. Norville, A.A. Yu, L. Wang, S. Trammell, L.E. Reddick, R. Kumar, S. Zhang, F. Stellacci, N. Lebedev, J. Schnur, B.D. Bruce and M. Baldo. Nano Letters. **4**. 1079-1083 (2004).

Photosynthetic complexes:

Molecularly activated bioswitches and agents for light powered molecular circuitry

Stephen Forrest, Princeton University, Princeton, NJ
Marc Baldo, Massachusetts Institute of Technology, Cambridge, MA

I. Personnel supported and/or associated with the research project

Graduate students: Jiangeng Xue (Princeton)
Barry Rand (Princeton)
Peter Peumans (Princeton)
Michael Segal (MIT)
Rajay Kumar (MIT)

Undergraduate students: Nicholas Stroustrup (Princeton)

II. Publications (only accepted or published publications listed)

1. "Integration of Photosynthetic Protein Molecular Complexes in Solid-State Electronic Devices", R. Das, P. Kiley, M. Segal, J. Norville, A. Yu, L. Wang, S. Trammell, L. Reddick, R. Kumar, F. Stellacci, N. Lebedev, J. Schnur, B. Bruce, S. Zhang, M. Baldo. *Nano Letters*, **1079** Vol. 4, No. 6 (2004)

III. Invention Disclosures for the AFOSR Program

1. Method for controlling electrodeposition of an entity
2. Devices incorporating the immobilized entity and solid state photosensitive devices

NANO LETTERS

2004
Vol. 4, No. 6
1079−1083

Integration of Photosynthetic Protein Molecular Complexes in Solid-State Electronic Devices

Rupa Das,[†] Patrick J. Kiley,[†,‡] Michael Segal,[†] Julie Norville,[†] A. Amy Yu,[§] Leyu Wang,[∥] Scott A. Trammell,[∥] L. Evan Reddick,[⊥] Rajay Kumar,[†] Francesco Stellacci,[§] Nikolai Lebedev,[∥] Joel Schnur,[∥] Barry D. Bruce,[⊥,#] Shuguang Zhang,[‡,▼] and Marc Baldo*[,†]

Department of Electrical Engineering and Computer Science, Center for Biomedical Engineering, Department of Materials Science and Engineering, and Center for Bits and Atoms, Massachusetts Institute of Technology, Cambridge, Massachusetts 02139, Center for Bio/Molecular Science and Engineering, U.S. Naval Research Laboratory, Washington, D.C. 20375, and Department of Biochemistry, Cellular and Molecular Biology, and Center of Excellence in Environmental Biotechnology, University of Tennessee, Knoxville, Tennessee 37996

Received March 15, 2004; Revised Manuscript Received April 21, 2004

ABSTRACT

Plants and photosynthetic bacteria contain protein−molecular complexes that harvest photons with nearly optimum quantum yield and an expected power conversion efficiency exceeding 20%. In this work, we demonstrate the integration of electrically active photosynthetic protein−molecular complexes in solid-state devices, realizing photodetectors and photovoltaic cells with internal quantum efficiencies of approximately 12%. Electronic integration of devices is achieved by self-assembling an oriented monolayer of photosynthetic complexes, stabilizing them with surfactant peptides, and then coating them with a protective organic semiconductor.

Photosynthetic complexes are archetypal molecular electronic devices, containing molecular optical and electronic circuitry organized by a protein scaffold. Conventional technology cannot equal the density of the molecular circuitry found in photosynthetic complexes.[1] Thus, if integrated with solid-state electronics, photosynthetic complexes might offer an attractive architecture for future generations of circuitry where molecular components are organized by a macromolecular scaffold. But like other protein molecular complexes, photosynthetic complexes are soft materials, optimized for operation in a lipid bilayer interface between aqueous solutions. For utilization in practical technological devices they must be stabilized and integrated with solid-state electronics.

In this work, we demonstrate a technique for integrating photosynthetic complexes with solid-state electronics. The generality of the technology is demonstrated by its application to two types of photosynthetic complexes. The simplest, and more robust, photosynthetic complex used is a bacterial reaction center (RC), isolated from the purple bacterium *Rhodobacter (Rb.) sphaeroides*. This RC consists of three protein subunits[2] labeled L, M, and H, that together coordinate six pigment molecules: a bacteriochlorophyll dimer known as the special pair, P, two monomer bacteriochlorophylls, B_L and B_M, two bacteriopheophytins, H_L and H_M, and two quinones, Q_a and Q_b. These molecules are symmetrically arranged in the L and M subunits,[2] but electron transfer is observed to occur principally through the L branch, and the quinone Q_b is the ultimate electron acceptor in the complex.[3] In addition to the *Rb. sphaeroides* RC, we also employ a much larger complex, Photosystem I (PSI), which is isolated here from spinach chloroplasts. Although its core is similar to the more primitive RC, PSI contains up to fourteen subunits.[4] Together with its associated light harvesting complexes, PSI coordinates approximately 200 chlorophyll molecules.[5] PSI also contains three Fe_4S_4 complexes that act as the terminal electron acceptors and reside outside of the transmembrane domain of the PSI complex.[5]

Two key technologies are employed to preserve the functionality of these photosynthetic complexes outside their

* Corresponding author. E-mail: baldo@mit.edu
[†] Department of Electrical Engineering and Computer Science, MIT.
[‡] Center for Biomedical Engineering, MIT.
[§] Department of Materials Science and Engineering, MIT.
[▼] Center for Bits and Atoms, MIT.
[∥] U.S. Naval Research Laboratory.
[⊥] Department of Biochemistry, Cellular and Molecular Biology, UT.
[#] Center of Excellence in Environmental Biotechnology, UT.

10.1021/nl049579f CCC: $27.50
Published on Web 05/19/2004

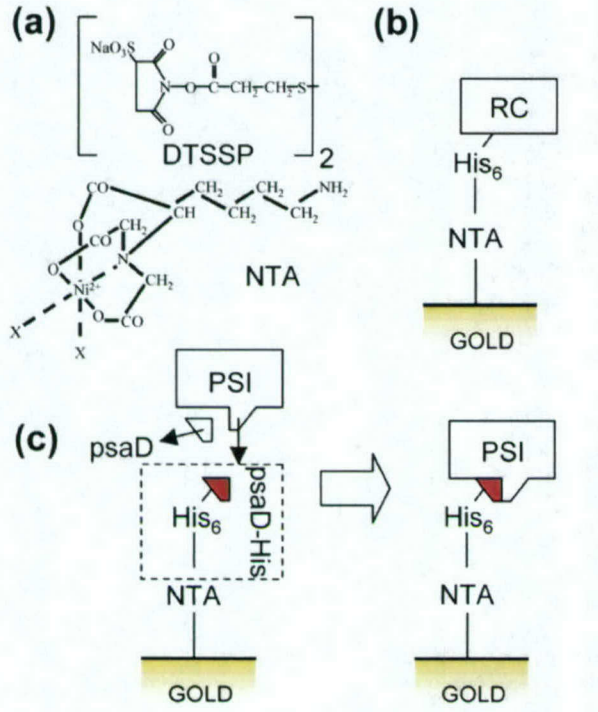

Figure 1. Techniques for oriented assembly of photosynthetic protein−molecular complexes. (a) To self-assemble oriented photosynthetic protein−molecular complexes, gold surfaces are first functionalized with DTSSP and then Ni^{2+}−NTA. (b) Bacterial reaction centers are immobilized using a His_6 tag at the C-terminal end of the M subunit. (c) Oriented PSI assembly is achieved when native psaD is exchanged with immobilized psaD-His, previously genetically modified with a His_6 tag.

native environment. To stabilize the photosynthetic complexes during device fabrication, we add two peptide surfactants, one cationic A_6K (AAAAAAK), and the other anionic V_6D (VVVVVVD).[6−9] Then we deposit a thin (<1000 Å) layer of an amorphous organic semiconductor between the photosynthetic complexes and a top metal contact. The use of thin films of organic semiconductors is established in photovoltaic applications[10] and they may be employed as solid-state antennae for photosynthetic complexes, thereby enhancing optical absorption.

Fabrication of devices proceeds as follows. Transparent and conductive indium−tin oxide (ITO)-coated glass[11] is used as the substrate for all photosensitive devices. A self-assembled monolayer of Ni^{2+}−NTA on ITO is used to orient photosynthetic components by selectively binding polyhistidine tags present on each complex;[12] see Figure 1. To facilitate chemical functionalization of the ITO surface, a thin, discontinuous 4 nm-thick film of gold is thermally evaporated on the ITO using a 1 nm-thick layer of Cr to promote adhesion. NTA functionalization of ITO/Au proceeds by first incubating with 6.1 mg/mL DTSSP for 10 min,[13] then after washing with deionized H_2O, incubating the surface with 0.33 mg/mL NTA ligand for 10 min.[14] Finally, the NTA-functionalized surface is charged with 200 mM nickel sulfate; see Figure 1a. Polyhistidine-tagged RCs are expressed and isolated from *Rb. sphaeroides* strain SMpHis with the tag constructed at the C-terminal end of

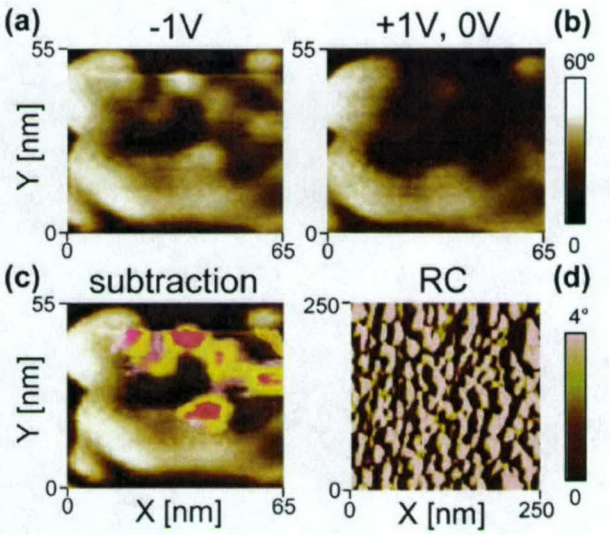

Figure 2. Characterization of self-assembled photosynthetic complexes by atomic force microscopy (AFM). The voltage dependence of a phase image of PSI particles is determined by applying a potential to the AFM tip. Note the phase changes in (a) the −1 V scan, relative to (b) the +1 V and 0 V scans. (c) Potential PSI particles are highlighted by superimposing a subtraction of the two images in (a) and (b) onto the −1 V scan. The voltage dependence confirms that the rectifying PSI complexes are oriented with the P700 dimer face up. (d) The phase profile of an assembled RC film showing a close-packed monolayer.

the RC M-subunit.[15] The expression and purification procedure was performed as described earlier.[16] RCs are then immobilized by incubating the functionalized ITO surface with approximately 100 μL of RC solution (0.2 mg/mL in 10 mM phosphate buffer pH 7.4, 0.05% LDAO and 0.02 M A_6K/V_6D (1:1)) for 1 h at 4 °C in the dark; see Figure 1b.

Native PSI complexes are isolated from spinach leaves as described earlier.[17] A single His_6 tag is introduced to isolated PSI complexes by engineering a protein subunit of PSI, psaD; see Figure 1c. First, the gene psaD from *Prochlorococcus marinus* is cloned into pET-21b between NdeI and XhoI, adding a C-terminal His_6 tag.[18] This recombinant psaD-His protein was expressed in *E. coli* (BL21 [DE3]) and purified by immobilized metal affinity chromatography. Next, the genetically modified protein (psaD-His) is immobilized on the Ni^{2+}−NTA functionalized ITO/Au surface and the unbound protein removed by washing. Finally, the surface is incubated with native PSI in 50 mM Tris, 25 mM NaCl, 2 M sucrose, 0.02% Triton X-100, and 0.02 M A_6K/V_6D (1:1) for 1 h at 4 °C in the dark. This incubation permits the intrinsic psaD subunit to be exchanged from the native PSI complexes and replaced by the immobilized psaD-His,[19] thereby immobilizing the PSI with its special pair oriented away from the ITO/Au substrate; see Figure 1d. It is believed that a similar exchange process occurs in vivo, allowing plants to replace photodamaged psaD.[19]

Tapping mode atomic force microscopy (TM-AFM) images of RC and PSI self-assembled monolayers on atomically flat Au-on-mica substrates are shown in Figure 2. To confirm the orientation of the PSI complexes we performed TM-AFM phase imaging in the intermittent contact mode and varied

the potential between the AFM tip and the ITO/Au substrate. The phase angle of the driven vibration of the cantilever in TM-AFM is related to the energy dissipated in the tip–sample interaction.[20] Thus, phase images of biological materials provide a map of the dissipative part of the sample's mechanical response. When a potential is applied to the AFM tip, we can alter its mechanical interactions with polar or charged samples by, for example, aligning polar molecules in the electric field. Voltage-dependent phase scans of a typical region of an assembled film are shown in Figure 2a and b. Phase scans taken at +1 V and 0 V show little difference, but phase scans taken at −1 V exhibit the appearance of localized regions of increased phase. A subtraction of the −1 V and 0 V images is superimposed on the −1 V image in Figure 2c. The increase in phase in the −1 V scan corresponds to an increase in the attractive forces between the tip and the sample[20] and indicates the presence of a positive charge trapped on the surface of PSI, mostly likely at the special pair, P700. Thus, the voltage dependence of TM-AFM phase imaging is consistent with the expected rectifying characteristics[21] of PSI in the orientation prescribed by self-assembly via exchange of psaD. PSI films formed using this method are less densely packed than the film of RC particles shown in Figure 2d.

The structures of the PSI and RC-based devices are shown in Figures 3a and b, respectively. To protect monolayers of PSI assembled on functionalized ITO we deposit via thermal evaporation at 10^{-6} Torr a thin coating of the archetype organic semiconductor tris(8-hydroxyquinoline) aluminum, Alq_3.[22] Alq_3 is transparent at the characteristic $\lambda = 680$ nm absorption peak of PSI. Alq_3 is also a preferentially electron-transporting material, thus under optical excitation at $\lambda =$ 680 nm, charges are generated primarily in PSI; electrons are transferred to the ITO substrate, holes are trapped on the special pair, P700, and the device acts as a photodetector. Fabrication of PSI-based devices is completed by deposition at 10^{-6} Torr of a 80-nm-thick film of Al deposited through a 1-mm-diameter shadow mask.

Owing to the topology of their respective polyhistidine tags, PSI and RC complexes are immobilized on the Ni^{2+}–NTA in opposite orientations. RCs are oriented with their electron-accepting special pair, P, facing the substrate. The RC-based photovoltaic cell shown in Figure 3b employs a 60 nm-thick protective layer of the preferentially electron transporting fullerene C60. C60 was chosen because of its relatively deep lowest unoccupied molecular orbital (LUMO) energy of 4.7 eV[23] that could enhance electron transfer from the electron acceptor Q_b in the RC. After C60, a 12 nm-thick layer of 2,9-dimethyl-4,7-diphenyl-1,10-phenanthroline (bathocuproine, or BCP)[22] is deposited. The thin BCP layer is damaged by subsequent deposition of an 80 nm thick Ag cathode through a 1 mm diameter shadow mask. Damage to BCP facilitates electron extraction[24] and the deep highest occupied molecular orbital (HOMO) of BCP effectively prevents the injection of holes into the device, markedly improving the device's reverse bias characteristics. Thermally evaporated films of C60, BCP, and Ag were deposited at a rate of $\approx$ 0.3 nm/s in a vacuum of $< 10^{-6}$ Torr.

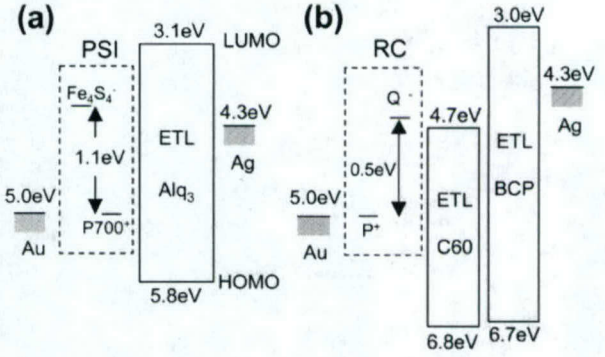

Figure 3. (a) Energy level diagram of a PSI photodetector. The highest occupied molecular orbital (HOMO) energy of the electron transport layer (ETL) Alq_3 is given by its ionization potential, extracted from ref 22. The relative $P700^+$ and $Fe_4S_4^-$ energy levels are taken from ref 1. (b) Energy level diagram of an RC photovoltaic cell. HOMO energies of the ETL's C60 and BCP are from refs 23 and 22, respectively. The relative P^+ and Q^- energy levels are taken from ref 1. Lowest unoccupied molecular orbital (LUMO) energies are estimated from the HOMO and the optical energy gap. It is assumed that no charge transfer occurs at the material interfaces.

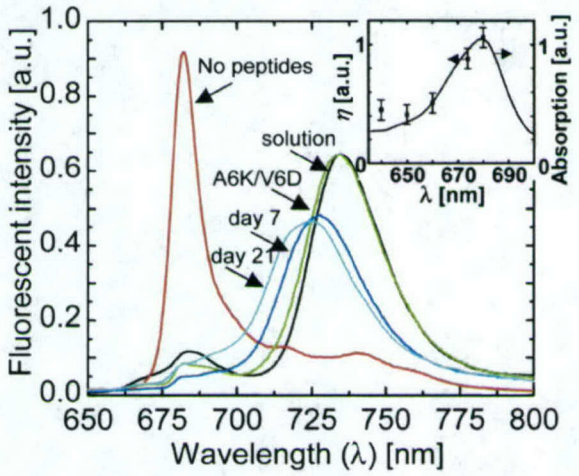

Figure 4. Comparison between the fluorescence spectrum of frozen ($T = 10$ K) PSI solution as extracted from spinach, with washed and dried films of PSI, demonstrates that PSI may be protected against degradation after washing and drying steps by stabilizing the complex with the surfactant peptides A_6K and V_6D. The stabilizing action of A_6K/V_6D is preserved for several weeks for dried films left in ambient conditions. (Inset) the stabilized PSI devices of Figure 3a exhibit a photocurrent spectrum that matches the absorption spectrum, confirming solid-state integration of stabilized PSI.

During device fabrication self-assembled monolayers of photosynthetic complexes must survive both a washing step, to remove surplus nonspecifically bound materials, and a drying step, to prepare the substrate for deposition of the semiconducting protective coating. The complexity and size of PSI makes it especially sensitive to degradation and dissociation.[25,26] The stability of PSI is assessed in Figure 4 using its fluorescent spectrum, which is enhanced at low temperatures. Thick, vacuum-dried films of PSI prepared without substrate functionalization were exposed to a pump laser at $\lambda = 408$ nm with intensity 0.5 mW/cm^2. At $T = 20$ K, in the absence of the stabilizing surfactant peptides, dried

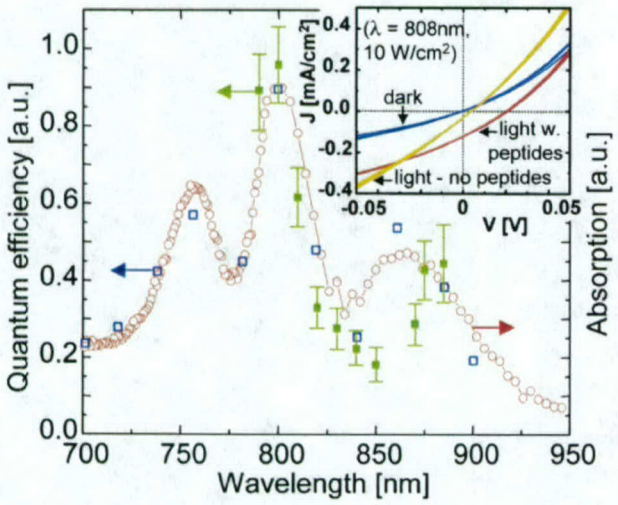

Figure 5. Photocurrent spectrum of photovoltaic devices employing bacterial reaction centers. A comparison between the photocurrent spectrum of solid-state (■) and wet electrochemical cell devices (□) and the solution absorption spectrum of the bacterial reaction centers (○), demonstrates that the observed photocurrent originates in the RCs. Wet cell device data is from ref 16. (Inset) stabilization of RC complexes with A_6K/V_6D peptides improves the internal quantum efficiency of the devices to 12% under short circuit conditions.

films of native PSI diluted in buffer exhibited significantly degraded fluorescence at $\lambda \approx 735$ nm. Polyelectrolytes such as poly(ethylene glycol), which may be used to preserve dried biological materials,[27] were similarly ineffective. In contrast, incubating PSI with A_6K/V_6D was found to almost entirely preserve the low-temperature fluorescent spectrum of PSI. The $\lambda = 735$ nm fluorescent peak of peptide-stabilized films stored in an ambient environment exhibited a gradual blue shift over several weeks, indicative of gradual structural changes in the light harvesting antennae of PSI.[28] In the inset of Figure 4, we show that the photocurrent spectrum of PSI−A_6K/V_6D devices exhibits the $\lambda = 680$ nm peak characteristic of the absorption spectrum of PSI, which, in conjunction with the low-temperature fluorescent data, demonstrates that PSI has been successfully integrated in a solid-state environment.

Unlike PSI, the activity of a significant fraction of the more robust RC complexes can be preserved, even in the absence of peptide surfactants. In Figure 5, the activity of an RC-based device without A_6K or V_6D is confirmed by spectrally resolving the short circuit current using a Ti−sapphire CW laser tunable between $\lambda = 790$ nm and $\lambda = 890$ nm. The photocurrent spectrum exhibits the characteristic peaks of both the solution absorption spectrum of the RC complexes, and a photocurrent spectrum of identical RC complexes in an electrochemical cell reproduced from ref 16. In the inset, we show the effect of A_6K/V_6D stabilization on the current−voltage characteristics of the devices. On average, the peptides were found to improve the open circuit voltage by a factor of 2−3.

The short circuit current density of the RC−A_6K/V_6D devices is 0.12 mA/cm^2 under an excitation intensity of 10 W/cm^2 at $\lambda = 808$ nm. Assuming a perfectly formed RC monolayer of density 3×10^{-12} mol/cm^2, and given an extinction coefficient of 2.9×10^5 M^{-1} cm^{-1},[29] we calculate the optimum photocurrent as 1 mA/cm^2, where we have ignored possible microcavity effects due to reflections from the ITO/Au electrode and assumed 100% reflection of the optical pump by the Ag cathode. Thus, under short-circuit conditions, a conservative estimate of the internal quantum efficiency of the device is 12%.

In conclusion, our results suggest that photosynthetic complexes may be used as an interfacial material in photovoltaic devices. Evolved within a thin membrane interface, photosynthetic complexes sustain large open circuit voltages of 1.1V[1] without significant electron−hole recombination, and they may be self-assembled into an insulating membrane, further reducing recombination losses. We have demonstrated here that they may be integrated in solid-state devices. Peptide surfactants have proved essential in stabilizing these complexes during and after device fabrication. Given typical quantum yields for photoinduced charge generation[1] of > 95% it is expected that the power conversion efficiency of a peptide-stabilized solid-state photosynthetic device may approach or exceed 20%. Similar integration techniques may applied to other biological or synthetic protein−molecular complexes.

Acknowledgment. The authors are grateful for discussions with Peter Peumans, and Elizabeth Broadwater for sample preparation. This work was funded by DARPA and AFOSR under contract F49620-02-1-0399 and in part by the MRSEC Program of the NSF under award DMR 02-13282. S.Z. acknowledges funding by MURI/AFOSR. Part of the data was taken with the assistance of Joe Gardecki using Laser Biomedical Research Center facilities supported by NIH grant P41 RR 02594 and Laser Research Facility supported by NSF grant 011137 CHE. Travel of B.D. Bruce was facilitated by a SARIF grant from UTK. Das and Kiley contributed equally to this work.

References

(1) Hoff, A. J.; Deisenhofer, J. *Phys. Rep.* **1997**, *287*, 1−247.
(2) Allen, J. P.; Feher, G.; Yeates, T. O.; Rees, D. C.; Deisenhoffer, J.; Michel, H.; Huber, R. *Proc. Nat. Acad. Sci. U.S.A.* **1986**, *83*, 8589−8593.
(3) Hörber, J. K. H.; Göbel, W.; Ogrodnik, A.; Michel-Beyerle, M. E.; Cogdell, R. J. *FEBS Lett.* **1986**, *198*, 268−272.
(4) Chitnis, P. R. *Annu. Rev. Plant Phys. Plant Mol. Biol.* **2001**, *52*.
(5) Ben-Shen, A.; Frolow, F.; Nelson, N. *Nature* **2003**, *426*, 630−635.
(6) Vauthey, S.; Santoso, S.; Gong, H.; Watson, N.; Zhang, S. *Proc. Natl. Acad. Sci. U.S.A.* **2002**, *99*, 5355−5360.
(7) Santoso, S.; Hwang, W.; Hartman, H.; Zhang, S. *Nano Lett.* **2002**, *2*, 687−691.
(8) von Maltzahn, G.; Vauthey, S.; Santoso, S.; Zhang, S. *Langmuir* **2003**, *19*, 4332−4337.
(9) Zhang, S. *Nature Biotechnol.* **2003**, *21*, 1171−1178.
(10) Tang, C. W. *Appl. Phys. Lett.* **1985**, *48*, 183−185.
(11) Applied Films, Boulder, Colorado.
(12) Smith, M. C.; Furman, T. C.; Ingolia, T. D.; Pidgeon, C. *J. Biol. Chem.* **1988**, *263*, 7211−7215.
(13) Katz, E. Y. *J. Electro. Chem.* **1990**, *291*, 257−260.
(14) Dithiobis(sulphosuccinimidyl propionate) (DTSSP) is obtained from Pierce Biotechnology, Rockford, IL. Nitrilotriacetic acid (NTA) ligand is obtained from Qiagen Inc., Valencia, CA.
(15) Goldsmith, J. O.; Boxer, S. G. *Biochim. Biophys. Acta* **1996**, *1276*, 171−175.
(16) Trammell, S. A.; Wang, L.; Zullo, J. M.; Shashidhar, R.; Lebedev, N. *Biosens. Bioelectron.* **2004**, *19*, 1649−1655.

(17) Bruce, B. D.; Malkin, R. *J. Biol. Chem.* **1988**, *263*, 7302−7308.
(18) pET-21B was obtained from Novagen, Madison, WI.
(19) Minai, L.; Fish, A.; Darash-Yahana, M.; Verchovsky, L.; Nechushtai, R. *Biochemistry* **2001**, *40*, 12754−12760.
(20) Cleveland, J. P.; Anczykowski, B.; Schmid, A. E.; Elings, V. B. *Appl. Phys. Lett.* **1998**, *72*, 2613−2615.
(21) Lee, I.; Lee, J. W.; Greenbaum, E. *Phys. Rev. Lett.* **1997**, *79*, 3294−3297.
(22) Hill, I. G.; Kahn, A. *J. Appl. Phys.* **1999**, *86*, 4515−4519.
(23) Dutton, G.; Zhou, X.-Y. *J. Phys. Chem. B* **2002**, *106*, 5975−5981.
(24) Peumans, P.; Forrest, S. *Appl. Phys. Lett.* **2001**, *79*, 126−128.
(25) Croce, R.; Zucchelli, G.; Garlaschi, F. M.; Bassi, R.; Jennings, R. C. *Biochemistry* **1996**, *35*, 8572−8579.
(26) Nechushtai, R.; Nourizadeh, S. D.; Thornber, J. P. *Biochim. Biophys. Acta* **1986**, *848*, 193−200.
(27) Mi, Y. L.; Wood, G.; Thoma, L.; Rashed, S. *PDA J. Pharm. Sci. Technol.* **2002**, *56*, 115−123.
(28) Morosinotto, T.; Breton, J.; Bassi, R.; Croce, R. *J. Biol. Chem.* **2003**, *278*, 49223−49229.
(29) Straley, S. C.; Parson, W. W.; Mauzerall, D. C.; Clayton, R. K. *Biochim. Biophys. Acta* **1973**, *305*, 597−609.

NL049579F